DMD Fast Forward. Published on October 25, 2021 as DOI: 10.1124/dmd.121.000644
This article has not been copyedited and formatted. The final version may differ from this version.

Title page

Intestinal UGT1A1 and protection against Irinotecan-induced toxicity in a novel UGT1A1 tissue-specific humanized mouse model

Elvira Mennillo, Xiaojing Yang, Andre A. Weber, Yoshihiro Maruo, Melanie Verreault, Olivier Barbier, Shujuan Chen, Robert H. Tukey

Laboratory of Environmental Toxicology, Department of Pharmacology, University of California San Diego, La Jolla, CA 92093 (E.M, X.Y., A.A.W., S.C., R.H.T.). Department of Pediatrics, Shiga University of Medical Science, Otsu, Shiga, Japan (Y.M.). Laboratory of Moléculaire Pharmacology, Centre de Recherche du CHU de Québec, Faculté of Pharmacie, Université Laval Québec, Québec, Canada (M.V., O.B.)

Address correspondence to: Robert H. Tukey, Department of Pharmacology, University of California, San Diego, 9500 Gilman Dr., CA 92093-0722. E-mail: rtukey@health.ucsd.edu

DMD Fast Forward. Published on October 25, 2021 as DOI: 10.1124/dmd.121.000644
This article has not been copyedited and formatted. The final version may differ from this version.

Running Title Page

Running Title: Humanized *UGT1A1* mice and irinotecan toxicity.

Corresponding author:

Robert H. Tukey, Department of Pharmacology, University of California, San Diego 9500 Gilman Drive, La Jolla, California, 92093-0722. E-mail: rtukey@health.ucsd.edu

Text pages: 18. (Abstract – Discussion, not including references and figure legends)

Tables: None

Figures: Five

Supplemental Figures: One

Abstract: 244

Introduction: 744

Discussion: 1187

Abbreviations

CC1, cleaved caspase 1; CC3, cleaved caspase 3; CC7, cleaved caspase 7; Cdkn1a, cyclin-dependent kinase inhibitor 1; CES, carboxylesterase; CHOP, C/EBP Homologous Protein; CPT-11, camptothecin/irinotecan; DPB, days post birth; *hUGT1* mice, human *UGT1* locus expressed in *Ugt1*$^{-/-}$ mice; *hUGT1A1*^{HEP} mice, human *UGT1A1* gene expressed in liver of *Ugt1*$^{-/-}$ mice; *hUGT1A1*^{GI} mice, human *UGT1A1* gene expressed in the gastrointestinal tract of *Ugt1*$^{-/-}$ mice; ER, endoplasmic reticulum; IEC, intestinal epithelium cell; ISCs, intestinal stem cells; SERCA, sarco/endoplasmic reticulum Ca^{2+} ATPase; SI, small intestine; SN-38, 7-ethyl-10-hydroxycamptothecin; SN-38G, SN-38 glucuronide; TGN, thapsigargin; TOP1, topoisomerase 1 TSB, total serum bilirubin; UGT, UDP-glucuronosyltransferase; UPR, unfolded protein response.

DMD Fast Forward. Published on October 25, 2021 as DOI: 10.1124/dmd.121.000644
This article has not been copyedited and formatted. The final version may differ from this version.

ABSTRACT

The human UDP-glucuronosyltransferases (UGTs) represent an important family of drug-metabolizing enzymes, with UGT1A1 targeting the conjugation and detoxification of many exogenous substances including pharmaceutical drugs. In this study we generated humanized UGT1A1 mice expressing the human *UGT1A1* gene in either liver (*hUGT1A1*^{HEP}) or intestine (*hUGT1A1*^{GI}), enabling experiments to examine tissue-specific properties of UGT1A1 specific glucuronidation. Hepatic and intestinal tissue-specific expression and function of UGT1A1 were demonstrated. Although the liver is considered a major organ for detoxification, intestinal UGT1A1 is an important contributor for drug clearance. Mice were challenged with irinotecan (CPT-11), a prodrug hydrolyzed by carboxylesterases to form the active metabolite SN-38 and detoxified by UGT1A1. Humanized *UGT1A1*^{HEP} mice, that have no intestinal UGT1A1, displayed a greater lethality rate when exposed to CPT-11 than *hUGT1A1*^{GI} mice. When exposed to a low dose of CPT-11 (10 mg/kg), *hUGT1A1*^{HEP} mice displayed greater intestinal inflammatory (IL-1β and IL-6) insult in addition to p53-triggered apoptotic responses. *In vitro* studies with intestinal crypt organoids exposed to CPT-11 confirmed the results observed *in vivo* and indicated that CPT-11 impacts stemness, apoptosis, and ER stress in organoids deficient UGT1A1. When we examined the induction of ER stress in organoids with thapsigargin (TGN), an inhibitor of sarco/endoplasmic reticulum Ca^{2+} ATPase (SERCA), apoptosis and the caspase surge that occurred in *hUGT1A1*^{HEP} mice were blocked in *hUGT1A1*^{GI} organoids. This study reveals the importance of intestinal UGT1A1 in preventing inflammation, apoptosis, and loss of stemness capacity upon systemic challenge with an important chemotherapeutic agent.

DMD Fast Forward. Published on October 25, 2021 as DOI: 10.1124/dmd.121.000644
This article has not been copyedited and formatted. The final version may differ from this version.

Significance Statement

Hepatic and intestinal UGT1A1 play a key role in the metabolism and detoxification of endogenous and exogenous compounds. The use of tissue-specific humanized models expressing UGT1A1 in liver or intestine has confirmed the relevance of the intestinal tract in the detoxification of irinotecan. Mechanistic studies using intestinal organoids highlighted the importance of UGT1A1 in reducing inflammation, apoptosis, and loss of stemness. These new models provide valuable tools for studying tissue-specific glucuronidation of substances that are metabolized by human UGT1A1.

DMD Fast Forward. Published on October 25, 2021 as DOI: 10.1124/dmd.121.000644
This article has not been copyedited and formatted. The final version may differ from this version.

INTRODUCTION

UDP-glucuronosyltransferases (UGTs) catalyze the conjugation of the glycosyl group of glucuronic acid to many of lipophilic endogenous and exogenous compounds (Tukey and Strassburg, 2000). The UGTs are involved in the metabolism and detoxifications of bile acids, steroids, hormones, environmental pollutants, chemical carcinogens, and a host of different xenobiotics (Tukey and Strassburg, 2000; Miners et al., 2004). The human UGTs have been documented to be expressed in a unique tissue specific pattern (Strassburg et al., 1997a; Strassburg et al., 1997b; Strassburg et al., 1998a; Strassburg et al., 1998b; Strassburg et al., 1999a; Strassburg et al., 1999b), providing an overall glucuronidation capacity that is unique to each tissue. Among the UGT1A subfamily of proteins (Mackenzie et al., 2005), UGT1A1 is of particular interest for its unique function in bilirubin clearance (Bosma et al., 1994). While UGT1A1 has a significant role in hepatic glucuronidation, it is present in many extrahepatic tissues, including the intestinal tract (Tukey and Strassburg, 2000). In humanized *UGT1* (*hUGT1*) mice, where we have expressed the human *UGT1* locus in a *Ugt1*$^{-/-}$ background, the *UGT1A* genes are expressed in a tissue specific pattern very similar to that observed in human tissues (Fujiwara et al., 2010; Fujiwara et al., 2018). Newborn *hUGT1* mice develop severe neonatal hyperbilirubinemia as a result of silenced liver gene expression and development delay in expression of intestinal UGT1A1, providing indirect evidence that intestinal expression is a significant event in bilirubin metabolism. The importance of intestinal expression was further confirmed following targeted deletion of the *Ugt1* locus in either the liver or gastrointestinal tract. Targeted deletion of the murine *Ugt1* locus in liver (*Ugt1*$^{\Delta HEP}$) led to mild induction of total serum bilirubin (2 mg/dl) in neonatal mice (Chen et al., 2013), compared to greater than 15 mg/dl in global *Ugt1*$^{-/-}$ mice (Nguyen et al., 2008) resulting in 100% neonatal lethality. These findings confirm that extrahepatic UGT1A1 metabolism plays an important role in controlling the

DMD Fast Forward. Published on October 25, 2021 as DOI: 10.1124/dmd.121.000644
This article has not been copyedited and formatted. The final version may differ from this version.

development of neonatal hyperbilirubinemia and demonstrates that bilirubin glucuronide can be actively excreted from intestinal epithelial cells into the lumen of the intestine.

Camptothecin (CPT)-11 (irinotecan) is a chemotherapeutic pro-drug used for the treatment of solid tumors. CPT-11 is the first-line therapeutic agent in the treatment of metastatic colorectal cancer, but its efficacy and safety can be compromised because of its severe side-effects, such as gastrointestinal injury/inflammation, severe diarrhea, and nausea (Ma and McLeod, 2003; Stein et al., 2010). Given intravenously, CPT-11 enters tissues such as the liver and intestinal tract and is hydrolyzed by carboxylesterase (CES) activity to the active topoisomerase 1 (TOP1) inhibitor, SN-38. Along with chemotherapeutic properties as a TOP1 inhibitor, free SN-38 is toxic and can disrupt cell function by inducing apoptosis. This toxicity is prevented by UGT1A1 glucuronidation of SN-38 to form the glucuronide (SN-38G). Following liver UGT1A1 glucuronidation, SN-38G is excreted into the bile and reaches the intestinal tract where it is susceptible to β-linkage cleavage producing free SN-38, where it can be reabsorbed into the intestinal tract. With glucuronidation of SN-38 in liver serving as a source of detoxification, the more SN-38G delivered to the intestinal tract the greater the absorption of SN-38 into the intestinal tract, providing a greater resource of TOP1 at the site of tumorigenesis. However, patients who carry the homozygous *UGT1A1*28* alleles, identified as Gilbert's syndrome, have reduced hepatic UGT1A1 expression (Tukey and Strassburg, 2000; Toffoli et al., 2006), would deliver less SN-38G through enterohepatic recirculation, yet are more sensitive towards the intestinal toxic actions of SN-38 (Toffoli et al., 2006; Palomaki et al., 2009).

The intestinal epithelium represents the fastest renewing tissue and the intestinal stem cells (ISCs) located in the deep bottom crypts play a crucial role in directing the renewal and regeneration of the villi-crypt structure (Umar, 2010). It is known that many chemotherapeutics cause enterotoxicity, a phenomenon that is usually associated with rapid crypt apoptosis (Keefe et al., 2000; Bowen et al., 2007). To examine the role of human UGT1A1 in SN-38 toxicity

DMD Fast Forward. Published on October 25, 2021 as DOI: 10.1124/dmd.121.000644
This article has not been copyedited and formatted. The final version may differ from this version.

protection, we have developed transgenic human UGT1A1 mouse models that express UGT1A1 in either the intestinal tract (*hUGT1A1*^{GI} mice) or in hepatocytes (*hUGT1A1*^{HEP}). Both *hUGT1A1*^{GI} and *hUGT1A1*^{HEP} mice were generated on a *Ugt1*-null background (Nguyen et al., 2008), allowing us to examine the contribution of liver and intestinal human UGT1A1 glucuronidation activity on the process of SN-38 elicited toxicity. We will assess the tissue-specific role of human UGT1A1 in CPT-11-induced intestinal toxicity by evaluating its impact on different aspects of intestinal physiology such as inflammation, apoptosis and ISC protection.

DMD Fast Forward. Published on October 25, 2021 as DOI: 10.1124/dmd.121.000644
This article has not been copyedited and formatted. The final version may differ from this version.

MATERIALS AND METHODS

Chemical Reagents. CPT-11 was supplied in 5-mL vials that contain 100 mg of irinotecan hydrochloride (20 mg/mL) under the trade name Camptosar ready-to-use solution by Pfizer. SN-38 glucuronide was obtained from Santa Cruz Biotechnology (Santa Cruz, CA). Thapsigargin (CAS no. 67526-95-8) was obtained from Sigma-Aldrich (St. Louis, MO, USA). Matrigel basement membrane matrix was purchased from Corning (Tewksbury, MA). Advanced DMEM/F12 medium and the supplements, including GlutaMax, HEPES, penicillin streptomycin, mouse EGF, N2, and B27 supplements, were purchased from Thermo Fisher Scientific (Waltham, MA); mouse Noggin was from PeproTech (Rocky Hill, NJ). HEK-293 cells producing R-Spondin 1 protein (293T-HA-Raspol_Fc cell line) was a generous gift from the Dr. Calvin Kuo laboratory at Stanford University (Ootani et al., 2009). The cells were cultured and passaged following a standard protocol. For collecting R-Spondin 1 conditioned media, 293T-HA-Raspol_Fc cells at approximately 75% confluency were changed to advanced DMEM/F12 medium and cultured for another week. Medium was then collected by passing through 0.22 mm sterile filter.

Generation of the Tissue-Specific UGT1A1 Mouse Models. To generate transgenic founders, plasmids containing human UGT1A1 cDNA driven by either a villin or albumin promoter were microinjected into pronuclei of fertilized mouse eggs and then were implanted in the oviduct of pseudo-pregnant recipient mouse. Pronuclear microinjection was performed by the Transgenic Mouse Core at UC San Diego. Transgenic (Tg) founders were identified by genotyping with specific primers (forward: AACAAGGAGCTCATGGCCTCC, reverse: GTTCGCAAGATTCGATGGTCG) and mated with *Ugt*$^{+/-}$ mice in a C57BL/6 background to obtain *TgUGT1A1*^{HEP}*/Ugt*$^{+/-}$ and *TgUGT1A1*^{GI}*/Ugt*$^{+/-}$ mice, respectively. Through backcrossing, we obtained fully humanized *TgUGT1A1*^{HEP}*/Ugt1*$^{-/-}$ (*hUGT1A1*^{HEP}) and *TgUGT1A1*^{GI}*/Ugt1*$^{-/-}$ (*hUGT1A1*^{GI}) mice (see Fig. 1A). All animals were housed at the University of California San

DMD Fast Forward. Published on October 25, 2021 as DOI: 10.1124/dmd.121.000644
This article has not been copyedited and formatted. The final version may differ from this version.

Diego (UCSD) Animal Care Facility. All the procedures and protocols were approved by the UCSD Animal Care and Use Committee (IACUC) and were conducted in accordance with federal regulations.

Bilirubin Measurements. Blood was collected from the submandibular vein and centrifuged at 16000g for 2 minutes. Serum samples were immediately measured for TSB levels using Unistat Bilirubinometer (Reichert, Depew, NY).

Animal Treatment with CPT-11. All mouse experiments and procedures were approved by the UCSD Animal Care and Use Committee (IACUC) and were conducted in accordance with federal regulations. For survival studies, four different doses of CPT-11 (50 mg/kg, 25 mg/kg, 15mg/kg and 10 mg/kg) were administered to mice once/day for 4 constitutive days by i.p. injection. Ten age-matched male mice (8 weeks old) per group were used for these experiments. For biological studies, 3-5 adult male mice per group were treated with 10 mg/kg of CPT-11 or PBS once/day for 4 consecutive days by i.p. injection and tissues collected on day 5 for further analysis.

Isolation of Crypt Cells, Organoid Cultures and Exposures. Intestinal crypt cell isolation and organoid culturing were carried out according to previous publications (Sato et al., 2009; Sato and Clevers, 2013) with several modifications. Mouse small intestine was dissected, cut longitudinally, and washed with ice-cold Dulbecco's phosphate-buffered saline (DPBS). The tissue was further dissected into small pieces and incubated in DPBS containing 2 mM EDTA at 4°C on a rocking tube platform for 30 minutes. The EDTA solution was removed, and 10% fetal bovine serum in DPBS buffer was added followed by vigorously shaking the tissue to release villi and crypt cells. The cell solution was filtered through a 70 mm cell strainer. The filtrate was centrifuged at 1000 g for 7 minutes at 4°C, and the cell pellet was resuspended in DPBS. Crypt cells were counted. Approximately 500 crypts were suspended into 25 µl ice-cold Matrigel and

DMD Fast Forward. Published on October 25, 2021 as DOI: 10.1124/dmd.121.000644
This article has not been copyedited and formatted. The final version may differ from this version.

plated into prewarmed 24-well culture plates. Twenty minutes after the incubation, 0.5 ml of complete growth medium (advanced DMEM with GlutaMax, HEPES, penicillin/streptomycin, N2 and B27 supplements, with 2.5mMN-acetylcysteine, 0.1 mg/ml mouse Noggin, 0.05 mg/ml mouse EGF, and 10% of R-Spondin1-conditioned medium) was added. The growth of crypt organoids was monitored. Mouse EGF was added every other day. Fresh medium was added every 3 days. Cells were normally ready for passage every 4-5 days. When passaging for maintenance, organoids were dissociated by vigorous pipetting. Organoids were exposed to various chemicals (CPT-11 and TGN) on day 3 and, after 24 hours, the cells were collected for further analysis. For the percent of malformed organoid assay cells were exposed on day 3 to TGN (0.1 μM) for 24 h and the malformed organoids were examined using 4x objective on inverted microscope Nikon ECLIPSE Ts2 with Nikon DS-F*i*3 camera, and data are expressed as percent (%) of malformed organoid relative to control (TGN 0 μM). RT-qPCR experiments were performed in triplicate. Western blot experiments were obtained from extracts pooled from three wells. Data are representative at least by two independent experiments.

Reverse Transcription Quantitative-PCR (RT-qPCR). Tissue samples and organoid cells were homogenized in 1mL TRIzol Reagent (Thermo Fisher Scientific) and total RNA from whole tissues was isolated using a previous protocol (Yoda *et al.*, 2017). Using iScript Reverse Transcriptase (Bio-Rad Laboratories, Hercules, CA), 1 μg of total RNA was used for the generation of cDNA in a total volume of 12 μL as outlined by the manufacturer. Following cDNA synthesis, quantitative PCR was carried out on a CFX96 qPCR system (BioRad) by using SsoAdvanced SYBR Green Supermix (BioRad). The list of primers used in this study is listed in Table S1.

Western blot analysis. Pulverized tissues (0.1 mg) and organoids were homogenized in 0.4 mL and 0.05 mL RIPA lysis buffer (EMD Millipore, Billerica, MA) supplemented with a protease and phosphatase inhibitor cocktail (Sigma-Aldrich), respectively. The samples were centrifuged

DMD Fast Forward. Published on October 25, 2021 as DOI: 10.1124/dmd.121.000644
This article has not been copyedited and formatted. The final version may differ from this version.

16,000g for 20 min at 4ºC and the supernatants were transferred to a new tube and kept at -80ºC until analysis. Western blots were performed by using NuPAGE 4–12% BisTris-polyacrylamide gels (Invitrogen) with the protocols described by the manufacturer. Protein (30 µg) was electrophoresed at 170 V for 60 min and transferred at 20 V for 60 min to PVDF membranes (EMD Millipore). Membranes were blocked with 5% non-fat milk at room temperature for 1 hour and incubated with primary antibodies, at 4 °C overnight. Membranes were washed and exposed to HRP-conjugated secondary antibodies (anti-mouse IgG, anti-rabbit IgG) for 1 hour at room temperature. Protein was detected by the ECL Plus Western blotting detection system (BioRad) and was visualized by the BioRad Chemidoc Touch Imaging System. Antibody used: UGT1A1 (Ab-170858), GAPDH (sc-32233), Cytochrome-c (11940; Cell Signaling), Cleaved Caspase-3 (9661; Cell Signaling), Cleaved Caspase 7 (9491; Cell Signaling), p53 (2524; Cell Signaling), Lgr5 (A10545; Abclonal), anti-mouse IgG horseradish peroxidase (HRP) conjugated antibody and anti-rabbit IgG HRP conjugated antibodies were obtained from Cell Signaling Technology, Inc. (Danvers, MA). All primary antibodies were diluted 1:1000, while secondary antibodies were diluted 1:3000. Band quantification of target proteins were quantified using Image Lab 5.2.1 software and normalized to GAPDH.

Histology Analysis. Mice were sacrificed and duodenum samples were dissected. Tissues were fixed for subsequent paraffin embedding. Paraffin-embedded sections were used for routine H&E staining, which were performed at the UCSD Cancer Center Histology Core. Slides were examined using a 20x Plan-Apochromat objective (numeric aperture, 0.8) on an upright Imager A2 microscope (Carl Zeiss Microscopy, LLC, White Plains, NY) with an Axiocam 506 color camera and ZEN2012 imaging software.

Glucuronidation Assays. Liver, small intestine and colon tissue (50 mg) homogenates were prepared in PBS-DTT 0.5 mM. Fifty µg of homogenates were then incubated in a previously reported glucuronidation assay buffer (Verreault et al., 2006) in the presence of SN-38 (10 mM)

DMD Fast Forward. Published on October 25, 2021 as DOI: 10.1124/dmd.121.000644
This article has not been copyedited and formatted. The final version may differ from this version.

for 30 minutes at 37°C. Following incubation, assays were quenched with 100 µl of MeOH-HCL 0.026M solution and centrifuged for 10 min at 13000 rpm. The formation of SN-38 glucuronide was quantified by liquid chromatography coupled to electrospray ionization - tandem mass spectrometry (LC/ESI-MS/MS) as previously reported (Lu et al., 2017), using a Synergi hydro-RP column (100X4.6mm, 4 µM; Phenomenex, Torrance, CA). The formation of glucuronide conjugates is expressed in ng/ml.

Statistical analyses. Data are represented as mean ± SEM. Statistical differences were determined by Student's t test (two groups), one-way ANOVA followed by Tukey's multiple comparison test (more than two groups). P values <0.05 were considered statistically significant, and statistically significant differences are indicated with *P<0.05; **P<0.01; ***P<0.001 and ****P<0.0001. Statistical analyses were performed using Prism 9 (GraphPad, San Diego, CA).

DMD Fast Forward. Published on October 25, 2021 as DOI: 10.1124/dmd.121.000644
This article has not been copyedited and formatted. The final version may differ from this version.

RESULTS

Tissue specific expression of UGT1A1. Neonatal *Ugt1*$^{-/-}$ mice, which are absent the functional UGT1A proteins including UGT1A1, develop severe neonatal hyperbilirubinemia with levels of unconjugated bilirubin that exceed 15 mg/dL (Nguyen et al., 2008), resulting in unconjugated bilirubin induced toxicity which is lethal 5-7 days after birth. In this study, we humanized *Ugt1*$^{-/-}$ mice with the human UGT1A1 cDNA. Expression of human UGT1A1 in either liver (*hUGT1A1*^{HEP}) or the gastrointestinal tract (*hUGT1A1*^{GI}) rescued the mice from the lethality caused by absence of *Ugt1a1* gene in *Ugt1*$^{-/-}$ mice. Both models displayed mild hyperbilirubinemia compared to *Ugt1*$^{-/-}$ mice at 7 days post birth (DPB) (Fig. S1 A). At 14 DPB, *hUGT1A1*^{GI} mice showed lower TSB levels than in *hUGT1A1*^{HEP} mice, while at 21 DPB both models exhibited TSB values that were near zero (Fig. S1 A). Western blot analysis revealed that human UGT1A1 protein expression is detected at day 3 in both mouse models, with higher UGT1A1 levels detected in the intestine of *hUGT1A1*^{GI} mice after 15 DPB compared to hepatic levels observed in *hUGT1A1*^{HEP} mice (Fig. S1 B). *hUGT1A1*^{GI} mice showed UGT1A1 mRNA and protein expression only in small intestine and colon, even though we found significantly lower levels in colon compared to the small intestine (Fig. 1B and C). On the contrary, *hUGT1A1*^{HEP} mice expressed UGT1A1 specifically in liver with undetectable levels of expression in small intestine and colon (Fig. 1B and C). Subsequently, the catalytic activity of UGT1A1 was examined using the exogenous substrate SN-38. The metabolism of SN-38 by glucuronidation follows the same metabolic pathway as bilirubin glucuronidation and is mainly metabolized by UGT1A1 (Ruggiero et al., 2009). The glucuronidation of SN-38 was measured in liver, small intestine, and colon tissues from *hUGT1A1*^{HEP} and *hUGT1A1*^{GI} mice (8 weeks old) (Fig. 1D). Expression of UGT1A1 in the GI tract resulted in SN-38G formation only in that tissue, with no activity in liver tissue. When we examined expression of UGT1A1 dependent SN-38 glucuronidation in *hUGT1A1*^{HEP} mice, SN-38G was only detected in liver tissue. TSB values at 8

DMD Fast Forward. Published on October 25, 2021 as DOI: 10.1124/dmd.121.000644
This article has not been copyedited and formatted. The final version may differ from this version.

weeks old were comparable between *hUGT1A1*^{HEP} and *hUGT1A1*^{GI} mice (Fig. 1E), with no differences in body weight between *hUGT1A1*^{HEP} and *hUGT1A1*^{GI} male mice and female mice (Fig. 1F). Expression of UGT1A1 in either the liver or intestines while serving as the only UGT1A protein in these mice had no impact on growth or reproduction and eliminated any potential TSB toxicity issues.

The impact of CPT-11 treatment. *hUGT1A1*^{HEP} and *hUGT1A1*^{GI} mice (8 weeks old) were treated with CPT-11 for 4 consecutive days. CPT-11-induced lethality was determined over a time course of 21 days and body weight monitored over a 15-day period. Survival curves and weight loss kinetics were generated for the different doses of CPT-11. When mice were treated with the 50 mg/kg dosage, Kaplan-Meier survival cures showed that this dose was lethal for all the *hUGT1A1*^{HEP} mice between days 6 and day 8 after the initial treatment, while *hUGT1A1*^{GI} mice had a survival rate of 20% (Fig. 2A). Weight loss was observed in both *hUGT1A1*^{HEP} and *hUGT1A1*^{GI} mice by 24h after the first administration. Significant differences were observed at day 7 when *hUGT1A1*^{HEP} mice reached an average loss of 35.9% compared to 19.6% registered in *hUGT1A1*^{GI} mice (Fig. 2B). The *hUGT1A1*^{GI} mice that survived the initial treatment recovered their weight loss within 15 days (Fig. 2B). When the dosage was reduced to 25 mg/kg, we observed a survival rate of ~40% in *hUGT1A1*^{GI} mice compared to 10% in *hUGT1A1*^{HEP} mice (Fig. 2C). The treatment with 25 mg/kg of CPT-11 did not show significant differences in terms of weight loss between the two mouse models, with highest loss (>25%) registered at day 7. However, the weight of the mice surviving the treatment recovered more slowly in the *hUGT1A1*^{HEP} mice than the *hUGT1A1*^{GI} mice (Fig. 2D). When CPT-11 dosage was further lowered to 15 mg/kg, *hUGT1A1*^{GI} mice showed a survival rate of 60% compared to 40% in *hUGT1A1*^{HEP} mice (Fig. 2E). At 15 mg/kg both models showed a similar weight loss range, although *hUGT1A1*^{HEP} mice had a significantly slower body weight recovery from day 11 (Fig. 2F). At the lowest dose of 10 mg/kg, *hUGT1A1*^{GI} mice displayed 90% survival against 80%

DMD Fast Forward. Published on October 25, 2021 as DOI: 10.1124/dmd.121.000644
This article has not been copyedited and formatted. The final version may differ from this version.

survival for *hUGT1A1*^{HEP} mice (Fig. 2G). At this concentration, both mouse models showed a weight loss lower than 20% with ≥80% of the mice surviving with a return to normal weight within 15 days (Fig. 2H). These findings confirm an important role for intestinal UGT1A1 in serving to protect against CPT-11 induced toxicity.

Intestinal UGT1A1 protects against CPT-11 induced inflammation and p53 dependent apoptosis. Based upon our dose response studies of CPT-11 measuring survival and the body weight loss, *hUGT1A1*^{HEP} and *hUGT1A1*^{GI} mice were treated with either phosphate buffered saline (PBS) or CPT-11 at 10 mg/kg for 4 consecutive days and were sacrificed on day 5 after the initial dose. Small intestinal tissue was collected for histology (H&E staining), RNA isolation and cellular protein preparations. As shown in Fig. 3A, H&E staining indicated that duodenum samples from CPT-11 treated *hUGT1A1*^{HEP} and *hUGT1A1*^{GI} mice presented moderate/severe damage with shortened villi compared to the control groups. However, the structure of the villi in CPT-11 treated *hUGT1A1*^{HEP} mice was severely damaged. Damage to the intestinal tract resulted in significantly decreased length in treated *hUGT1A1*^{HEP} mice (Fig. 3B) when compared to *hUGT1A1*^{GI} mice. The accelerated intestinal toxicity in *hUGT1A1*^{HEP} mice was presented with a higher rate of tissue inflammation, as evident from increased *Il-6* and *Il-1β* (Fig. 3C and D).

CPT-11 and other anticancer drugs alter cell cycle control as well as cellular apoptosis, thus suppressing tumor development. In *hUGT1A1*^{HEP} mice treated with CPT-11, there was a significant induction of cyclin-dependent kinase inhibitor 1 (*Cdkn1a*), a p53 downstream gene (Fig. 3E), which would prevent phosphorylation of cyclin-dependent kinase substrates leading to blockage of cell cycle progression. CPT-11 treatment leads to induction of p53 in the intestinal tissue of both *hUGT1A1*^{HEP} and *hUGT1A1*^{GI} mice, but the induction resulted in far greater p53 expression in *hUGT1A*^{HEP} mice where there was no expression of UGT1A1, which was necessary to protect the tissue against SN-38 toxicity. In line with p53 induction, the apoptotic biomarkers caspase-3 and -7 were also induced in *hUGT1A1*^{HEP} mice along with cleaved

DMD Fast Forward. Published on October 25, 2021 as DOI: 10.1124/dmd.121.000644
This article has not been copyedited and formatted. The final version may differ from this version.

caspase-1 (CC1) (Fig. 3F and G). The release of cytochrome-c from the mitochondrial into the cytosol is known to activate the apoptotic intrinsic pathway. When we examined cytochrome-c protein expression, it was found more abundant in the small intestine from *hUGT1A1*^{HEP} mice treated with CPT-11 than *hUGT1A1*^{GI} mice (Fig. 3F and G). The health of the intestinal tract is based upon the ability of the tissue to regenerate new intestinal epithelial cells (IECs), which originate from stem cells at the base of the intestinal crypts. When we examined Lgr5 protein expression, a selective marker of intestinal stem cells, there was reduced expression in the intestinal tissue from CPT-11 treated *hUGT1A1*^{HEP} mice, indicating that CPT-11 treatment impacts the regeneration of the absorptive and secretory IEC pathways (Fig. 3F and G).

The impact of CPT-11 exposure to *hUGT1A1*^{HEP} and *hUGT1A1*^{GI} *organoids*. To gain insight into the effects of CPT-11 toxicity in presence/absence of UGT1A1, we isolated crypt organoids from both *hUGT1A1*^{GI} and *hUGT1A1*^{HEP} mice (Fig. 4A). The mouse model characteristics were maintained *in vitro*, as UGT1A1 gene and protein expression were found only in the *hUGT1A1*^{GI} strain (Fig. 4B). Organoids were exposed to serial concentrations of CPT-11 for 24 hours. A greater degree of inflammatory insult, as measured by *Tnfα* and *Cdkn1a* gene expression (Fig. 4C and D), was statistically more significant in organoids that were absent intestinal UGT1A1 (*hUGT1A1*^{HEP} mice). With the lower doses of CPT-11 (0.1-1.0 μM), there is far greater reduction in the deep crypt biomarker *Lgr5* in *hUGT1A1*^{HEP} organoids, indicating toxicity is being protected by UGT1A1. However, at 10 μM CPT-11, Lgr5 expression was equally impacted in organoids from both *hUGT1A1*^{GI} and *hUGT1A1*^{HEP} mice, indicating that this dose overrides the protective effects of UGT1A1 expression. The changes observed in inflammatory markers and stem cell marker following CPT-11 exposure is also reflected in evidence of greater apoptosis. At 0.1 and 1 μM CPT-11 exposures, Caspase-3 cleavage was sensitive in *hUGT1A1*^{HEP} mice, in addition to increased protein expression of cytochrome-c (Fig. 4F and G). Matching gene expression, Western blot analysis confirms greater expression of Lgr5 in *hUGT1A1*^{GI} mice than in

DMD Fast Forward. Published on October 25, 2021 as DOI: 10.1124/dmd.121.000644
This article has not been copyedited and formatted. The final version may differ from this version.

hUGT1A1^{HEP} mice, lending additional support to the findings that UGT1A1 expression protects against CPT-11 toxicity.

Implications that UGT1A1 protects against endoplasmic reticulum (ER) induced apoptosis. Our findings regarding CPT-11 induced apoptosis in intestinal tissue from *hUGT1A1*^{GI} and *hUGT1A1*^{HEP} mice with cleavage of Caspase-3 and -7 along with increased expression of Cytochrome C implicates activation of ER stress and induced apoptosis (Hu et al., 2019). These events are protected in *hUGT1A1*^{GI} mice, a result that can be linked to the metabolism of SN-38 by UGT1A1. To examine more specifically the actions of ER stress, intestinal organoids from *hUGT1A1*^{GI} and *hUGT1A1*^{HEP} mice were treated with thapsigargin (TGN), an inhibitor of sarco/endoplasmic reticulum Ca^{2+} ATPase (SERCA). Calcium depletion in the ER leads to ER stress, activation of the unfolded protein response (UPR) and apoptosis (Denmeade and Isaacs, 2005). A central mediator of ER stress regulated apoptosis induced by caspase activation and mitochondria damage is the transcription factor C/EBP Homologous Protein (CHOP), when activated can induce apoptosis through several different regulatory pathways (Hu et al., 2019). The induction of ER stress following TGN treatment leads to disorganization of the organoids, with greater disruption in *hUGT1A1*^{HEP} mice (Fig. 5A). When we examined *Chop* and *Atf5* gene expression following TGN exposure, there was considerable induction in organoids from *hUGT1A1*^{GI} and *hUGT1A1*^{HEP} mice that was elicited through a dose response effect, with greater induction in *hUGT1A1*^{HEP} mice (Fig. 5B and C). TGN was found to also impact on cellular stemness, as suggested by a decrease of *Lgr5* expression in both models (Fig. 5D). Western blot analysis of protein biomarker levels indicated stronger apoptosis (Cleaved Casp-3 and -7) in *hUGT1A1*^{HEP} mice. However, Caspase-3 and -7 activation, the major signaling events underlying the caspase surge, was dramatically reduced in the organoids from *hUGT1A1*^{GI} mice that express UGT1A1 (Fig. 5E and F). This surprising result indicates that expression of UGT1A1 plays an important role in stabilizing the downstream effects of ER

DMD Fast Forward. Published on October 25, 2021 as DOI: 10.1124/dmd.121.000644
This article has not been copyedited and formatted. The final version may differ from this version.

stress, supporting previous studies that the lack of the UGT1A proteins causes higher intestinal ER stress (Liu et al., 2016). Thus, the protection afforded the intestinal tract by expression of UGT1A1 may serve a dual role. First, UGT1A1 is involved in the metabolism of SN-38, preventing intestinal tissue damage. Second, UGT1A1 plays a role in stabilizing the ER, in a mechanism that is currently not defined, leading to reduced cell damage and apoptosis.

DMD Fast Forward. Published on October 25, 2021 as DOI: 10.1124/dmd.121.000644
This article has not been copyedited and formatted. The final version may differ from this version.

Discussion

Molecular and immunohistochemical studies evaluating UGT expression patterns have shown that UGT1A1 along with other UGT1As are present in human small and large intestine, and colon epithelial cells (Strassburg et al., 1998a; Strassburg et al., 1999a, (Strassburg et al., 2000). Two tissue-specific humanized animal models expressing UGT1A1 in liver (*hUGT1A1*^{HEP}) or intestine (*hUGT1A1*^{GI}) have been developed in a *Ugt1* null background. Previous studies using humanized UGT1 (*hUGT1*) mice showed that the expression of the *UGT1A1* gene rescued early neonatal lethality observed in *Ugt1*$^{-/-}$ mice (Chen et al., 2005; Nguyen et al., 2008; Fujiwara et al., 2010). The presence of human UGT1A1 in liver or intestine rescued these mice from bilirubin toxicity and death, demonstrating that metabolism of bilirubin in either tissue is sufficient for clearance of serum bilirubin. This finding supports previous findings from our laboratory when we demonstrated that the deletion of the murine *Ugt1* locus in liver tissue had little impact on overall metabolism of serum bilirubin (Chen et al., 2013), supporting the concept that extra hepatic bilirubin metabolism is sufficient to protect against bilirubin toxicity. This evidence supports the importance of intestinal UGT1A1 in bilirubin clearance, as originally indicated with the *hUGT1* mouse model (Fujiwara et al., 2010). We had previously reported that in neonatal intestine, the expression of UGT1A1 distributes quite evenly in both the longitudinal axis and the crypt-villi axis. We also demonstrated that UGT1A1 expression was significantly upregulated following the villin-Cre driven IEC specific deletion of nuclear receptor corepressor NCoR1. These results support that UGT1A1 expression is IEC-enriched for villin promoter driven UGT1A1 expression mimics the physiological condition associated with expression of human UGT1A1.

Along with the unique role that UGT1A1 plays in bilirubin metabolism, UGT1A1 is also fundamental for the detoxification of many environmental toxicants, xenobiotics, and drugs (Kiang et al., 2005; Lv et al., 2019). A key example of this is the detoxification of the

DMD Fast Forward. Published on October 25, 2021 as DOI: 10.1124/dmd.121.000644
This article has not been copyedited and formatted. The final version may differ from this version.

chemotherapeutic drug Camptothecin (CPT)-11 (Irinotecan), a pro-drug that is metabolized by carboxylesterase activity in tissues to the active topoisomerase inhibitory metabolite SN-38, which is then inactivated by UGT1A1 dependent glucuronidation. The effectiveness of CPT-11 as a solid tumor chemotherapeutic agent towards colon cancer has been exploited since delivery of SN-38 to the tissue occurs both through enterohepatic circulation and directly through absorption of CPT-11 from the basolateral surface. For many years, the metabolism and detoxification of SN-38 have been linked primarily to hepatic metabolism, with clinical findings in Gilbert's patients being at greater risk of CPT-11 induced colon toxicity. The toxicity affiliated with Gilbert's syndrome has been linked to reduced expression UGT1A1 in hepatic tissue. However, this rationale is flawed since the concentrations of SN-38G excreted into the intestinal tract from the liver in Gilbert's would be substantially less than in normal patients. One would have to speculate that under clinically relevant concentrations of CPT-11 in Gilbert's syndrome, reduced metabolism of SN-38 in liver would leave greater concentrations of systemic CPT-11 available for absorption into the colon. For toxicity to develop, glucuronidation of SN-38 would have to be saturated. This has never been demonstrated, and the underlying importance of human UGT1A1 in liver and intestine as a modulator of CPT-11 efficacy has not been mechanistically elucidated.

Expression of human UGT1A1 in the either the intestinal tract or liver results in sufficient glucuronidation of SN-38 using whole tissue extracts, indicating that human UGT1A1 will metabolize SN-38 in vivo following the administration of CPT-11. Dose response analysis of CPT-11 documenting weight loss and overall survival has confirmed that expression of UGT1A1 in the intestinal tract protects from CPT-11 toxicity. While our lowest dose of CPT-11 (10 mg/kg) showed little difference in weight loss or survival in comparing *hUGT1A1*^{GI} and *hUGT1A1*^{HEP} mice, this dose displayed significant induction of intestinal inflammatory cytokines, histological damage to the villi, shortening of the intestinal tract, and induction of pro-apoptotic proteins

DMD Fast Forward. Published on October 25, 2021 as DOI: 10.1124/dmd.121.000644
This article has not been copyedited and formatted. The final version may differ from this version.

when UGT1A1 is absent (*hUGT1A1*^{HEP} mice). SN-38 has been shown to increase DNA damage via activation of p53 (Takeba et al., 2007), and this occurs in intestinal tissue in the absence of UGT1A1. These findings are associated with increased release of mitochondrial cytochrome-c into the cytosol, all factors that facilitate the activation of effector caspases such as caspase-3 and -7. Although, caspase-3 and -7 are known to display functional overlap, several observations have suggested their non-redundant role in apoptosis (Slee *et al.*, 2001; Walsh *et al.*, 2008). Indeed, biochemical evidence showed that caspase-7 is a direct substrate of caspase-1 (Lamkanfi et al., 2008), supporting the role of caspase-7 during the inflammation process (Lamkanfi and Kanneganti, 2010). These findings document that when intestinal UGT1A1 is reduced, low concentrations of CPT-11 can stimulate intestinal inflammation and apoptosis and further tissue damage. If metabolism of accumulating concentrations of intestinal SN-38 is critical to combat the toxic actions of CPT-11 treatment, therapeutic induction of intestinal UGT1A1 through PXR (Chen et al., 2012), CAR (Cai et al., 2010), LXRα (Hansmann et al., 2020) or PPARα (Senekeo-Effenberger et al., 2007) using selective nuclear receptor agonists prior to CPT-11 chemotherapy may reduce intestinal toxicity.

We have shown previously that deletion of the murine *Ugt1* locus (*Ugt1*$^{\Delta IEC}$ mice) in wild type mice sensitizes intestinal organoids towards exposure to increasing concentrations of CPT-11. With *hUGT1A1* mice, deletion of UGT1A1 in intestinal organoids leaves them more susceptible to CPT-11 induced inflammation and apoptosis. Very low levels of CPT-11 (0.1 μM) lead to dramatic activation of activated Casp-3 and Casp-7, with a reduction in the deep crypt marker Lgr5. This finding indicates that very low concentrations CPT-11 are capable of altering stem cell function, which is critical for the generation and regeneration of intestinal epithelial cells that are aligned with either the absorptive or secretory lineage. The induction of activated Casp-3 and Casp-7 along with reduction in stemness in *hUGT1A1*^{HEP} organoids indicates that CPT-11 is inducing ER stress. To compare the impact of CPT-11 on *hUGT1A1*^{HEP} and

DMD Fast Forward. Published on October 25, 2021 as DOI: 10.1124/dmd.121.000644
This article has not been copyedited and formatted. The final version may differ from this version.

hUGT1A1^{GI} organoids with agents known to induce ER stress, the organoids were treated with TGN, which induces ER stress through loss of calcium. Key markers associated with apoptosis, inflammation, and stemness were like those characterized when organoids were treated with CPT-11. Of particular interest was the observation that the induction of ER stress by TGN was much more resistant in organoids isolated from *hUGT1A1*^{GI} mice, as highlighted by gene expression of *Atf5* and *Chop*. Since UGT1A1 does not target the metabolism of TGN, this finding indicates that the physical presence of UGT1A1 in the ER is important in resisting the onset of ER stress. There is precedence that the presence of the UGT1A proteins plays a key role in protecting against ER stress, as we had demonstrated previously confirming that deletion of the *Ugt1* locus in intestines (*Ugt1*$^{\Delta IEC}$ mice) potentiated ER stress following the induction of ulcerative colitis by dextran sodium sulfate treatment (Liu et al., 2016). Thus, expression of intestinal UGT1A1 serves a dual purpose in intestinal tissue following CPT-11 treatment; it serves to metabolize SN-38 to limit toxicity while it also prevents the onset of ER stress. These findings indicate that overexpression of UGT1A1 in intestinal tissue may be highly beneficial for the efficacy of CPT-11 treatment while also preventing severe intestinal toxicity.

Acknowledgments

Author Contributions

Designed the experiments: Mennillo, Maruo, Chen, Barbier, and Tukey

Initial concept: Tukey

Performed the experiments: Mennillo, Weber, Yang, Maruo, Verreault

Wrote the manuscript: Mennillo and Tukey

DMD Fast Forward. Published on October 25, 2021 as DOI: 10.1124/dmd.121.000644
This article has not been copyedited and formatted. The final version may differ from this version.

References

Bosma PJ, Seppen J, Goldhoorn B, Bakker C, Oude ER, Chowdhury JR, Chowdhury NR, and Jansen PL (1994) Bilirubin UDP-glucuronosyltransferase 1 is the only relevant bilirubin glucuronidating isoform in man. *J Biol Chem* **269:**17960-17964.

Bowen JM, Gibson RJ, Stringer AM, Chan TW, Prabowo AS, Cummins AG, and Keefe DM (2007) Role of p53 in irinotecan-induced intestinal cell death and mucosal damage. *Anticancer Drugs* **18:**197-210.

Cai H, Nguyen N, Peterkin V, Yang YS, Hotz K, Beaton La PD, Chen S, Tukey RH, and Stevens JC (2010) A Humanized *UGT1* Mouse Model Expressing the *UGT1A1*28* Allele for Assessing Drug Clearance by UGT1A1 Dependent Glucuronidation. *Drug Metab Dispos* **38:**879-886.

Chen S, Operana T, Bonzo J, Nguyen N, and Tukey RH (2005) ERK kinase inhibition stabilizes the aryl hydrocarbon receptor: implications for transcriptional activation and protein degradation. *J Biol Chem* **280:**4350-4359.

Chen S, Yueh MF, Bigo C, Barbier O, Wang K, Karin M, Nguyen N, and Tukey RH (2013) Intestinal glucuronidation protects against chemotherapy-induced toxicity by irinotecan (CPT-11). *Proc Natl Acad Sci U S A* **110:**19143-19148.

Chen S, Yueh MF, Evans RM, and Tukey RH (2012) The Pregnane-X-receptor controls hepatic glucuronidation during pregnancy and neonatal development in humanized UGT1 Mice. *Hepatology* **56:**658-667.

Denmeade SR and Isaacs JT (2005) The SERCA pump as a therapeutic target: making a "smart bomb" for prostate cancer. *Cancer biology & therapy* **4:**14-22.

Fujiwara R, Nguyen N, Chen S, and Tukey RH (2010) Developmental hyperbilirubinemia and CNS toxicity in mice humanized with the UDP glucuronosyltransferase 1 (*UGT1*) locus. *Proc Natl Acad Sci U S A* **107:**5024-5029.

Fujiwara R, Yoda E, and Tukey RH (2018) Species differences in drug glucuronidation: Humanized UDP-glucuronosyltransferase 1 mice and their application for predicting drug glucuronidation and drug-induced toxicity in humans. *Drug Metab Pharmacokinet* **33:**9-16.

Hansmann E, Mennillo E, Yoda E, Verreault M, Barbier O, Chen SJ, and Tukey RH (2020) Differential role of LXRalpha and LXRbeta in the regulation of UDP-glucuronosyltransferase 1A1 in humanized UGT1 mice. *Drug Metab Dispos*.

Hu H, Tian M, Ding C, and Yu S (2019) The C/EBP Homologous Protein (CHOP) Transcription Factor Functions in Endoplasmic Reticulum Stress-Induced Apoptosis and Microbial Infection. *Frontiers in Immunology* **9**.

Keefe DM, Brealey J, Goland GJ, and Cummins AG (2000) Chemotherapy for cancer causes apoptosis that precedes hypoplasia in crypts of the small intestine in humans. *Gut* **47:**632-637.

Kiang TK, Ensom MH, and Chang TK (2005) UDP-glucuronosyltransferases and clinical drug-drug interactions. *Pharmacol Ther* **106:**97-132.

Lamkanfi M and Kanneganti TD (2010) Caspase-7: a protease involved in apoptosis and inflammation. *Int J Biochem Cell Biol* **42:**21-24.

Lamkanfi M, Kanneganti TD, Van Damme P, Vanden Berghe T, Vanoverberghe I, Vandekerckhove J, Vandenabeele P, Gevaert K, and Núñez G (2008) Targeted peptidecentric proteomics reveals caspase-7 as a substrate of the caspase-1 inflammasomes. *Molecular & cellular proteomics : MCP* **7:**2350-2363.

Liu M, Chen S, Yueh MF, Wang G, Hao H, and Tukey RH (2016) Reduction of p53 by knockdown of the locus in colon epithelial cells causes an increase in tumorigenesis. *Cell Mol Gastroenterol Hepatol* **2:**63-76.

Lv X, Xia Y, Finel M, Wu J, Ge G, and Yang L (2019) Recent progress and challenges in screening and characterization of UGT1A1 inhibitors. *Acta Pharm Sin B* **9:**258-278.

Ma MK and McLeod HL (2003) Lessons learned from the irinotecan metabolic pathway. *Curr Med Chem* **10:**41-49.

Mackenzie PI, Walter BK, Burchell B, Guillemette C, Ikushiro S, Iyanagi T, Miners JO, Owens IS, and Nebert DW (2005) Nomenclature update for the mammalian UDP glycosyltransferase (UGT) gene superfamily. *Pharmacogenet Genomics* **15:**677-685.

Miners JO, Smith PA, Sorich MJ, McKinnon RA, and Mackenzie PI (2004) Predicting human drug glucuronidation parameters: application of in vitro and in silico modeling approaches. *Annu Rev Pharmacol Toxicol* **44:**1-25.

Nguyen N, Bonzo JA, Chen S, Chouinard S, Kelner M, Hardiman G, Belanger A, and Tukey RH (2008) Disruption of the *Ugt1* locus in mice resembles human Crigler-Najjar type I disease. *J Biol Chem* **283:**7901-7911.

Ootani A, Li X, Sangiorgi E, Ho QT, Ueno H, Toda S, Sugihara H, Fujimoto K, Weissman IL, Capecchi MR, and Kuo CJ (2009) Sustained in vitro intestinal epithelial culture within a Wnt-dependent stem cell niche. *Nat Med* **15:**701-706.

Palomaki GE, Bradley LA, Douglas MP, Kolor K, and Dotson WD (2009) Can UGT1A1 genotyping reduce morbidity and mortality in patients with metastatic colorectal cancer treated with irinotecan? An evidence-based review. *Genet Med* **11:**21-34.

Ruggiero A, Coccia P, Scalzone M, Attina G, and Riccardi R (2009) Treatment of childhood sarcoma with irinotecan: bilirubin level as a predictor of gastrointestinal toxicity. *J Chemother* **21:**693-697.

Sato T and Clevers H (2013) Growing self-organizing mini-guts from a single intestinal stem cell: mechanism and applications. *Science* **340:**1190-1194.

Sato T, Vries RG, Snippert HJ, van de Wetering M, Barker N, Stange DE, van Es JH, Abo A, Kujala P, Peters PJ, and Clevers H (2009) Single Lgr5 stem cells build crypt-villus structures in vitro without a mesenchymal niche. *Nature* **459:**262-265.

Senekeo-Effenberger K, Chen S, Brace-Sinnokrak E, Bonzo JA, Yueh MF, Argikar U, Kaeding J, Trottier J, Remmel RP, Ritter JK, Barbier O, and Tukey RH (2007) Expression of the Human UGT1 Locus in Transgenic Mice by 4-Chloro-6-(2,3-xylidino)-2-pyrimidinylthioacetic Acid (WY-14643) and Implications on Drug Metabolism through Peroxisome Proliferator-Activated Receptor a Activation. *Drug Metabolism and Disposition* **35:**419-427.

Stein A, Voigt W, and Jordan K (2010) Chemotherapy-induced diarrhea: pathophysiology, frequency and guideline-based management. *Therapeutic advances in medical oncology* **2:**51-63.

Strassburg CP, Kneip S, Topp J, Obermayer-Straub P, Barut A, Tukey RH, and Manns MP (2000) Polymorphic gene regulation and interindividual variation of UDP-glucuronosyltransferase activity in human small intestine. *J Biol Chem* **275:**36164-36171.

Strassburg CP, Manns MP, and Tukey RH (1997a) Differential down regulation of the *UDP-glucuronosyltransferase 1A* locus is an early event in human liver and biliary cancer. *Cancer Res* **57:**2979-2985.

Strassburg CP, Manns MP, and Tukey RH (1998a) Expression of the *UDP-glucuronosyltransferase 1A* locus in human colon. Identification and characterization of the novel extrahepatic UGT1A8. *J Biol Chem* **273:**8719-8726.

Strassburg CP, Nguyen N, Manns MP, and Tukey RH (1998b) Polymorphic expression of the UDP-glucuronosyltransferase *UGT1A* gene locus in human gastric epithelium. *Molecular Pharmacology* **54:**647-654.

Strassburg CP, Nguyen N, Manns MP, and Tukey RH (1999a) UDP-glucuronosyltransferase activity in human liver and colon. *Gastroenterology* **116:**149-160.

Strassburg CP, Oldhafer K, Manns MP, and Tukey RH (1997b) Differential expression of the *UGT1A* locus in human liver, biliary, and gastric tissue: identification of UGT1A7 and UGT1A10 transcripts in extrahepatic tissue. *Mol Pharmacol* **52:**212-220.

Strassburg CP, Strassburg A, Nguyen N, Li Q, Manns MP, and Tukey RH (1999b) Regulation and function of family 1 and family 2 UDP- glucuronosyltransferase genes (*UGT1A, UGT2B*) in human oesophagus. *Biochem J* **338 (Pt 2):**489-498.

Takeba Y, Kumai T, Matsumoto N, Nakaya S, Tsuzuki Y, Yanagida Y, and Kobayashi S (2007) Irinotecan activates p53 with its active metabolite, resulting in human hepatocellular carcinoma apoptosis. *J Pharmacol Sci* **104:**232-242.

Toffoli G, Cecchin E, Corona G, Russo A, Buonadonna A, D'Andrea M, Pasetto LM, Pessa S, Errante D, De P, V, Giusto M, Medici M, Gaion F, Sandri P, Galligioni E, Bonura S, Boccalon M, Biason P, and Frustaci S (2006) The role of UGT1A1*28 polymorphism in the pharmacodynamics and pharmacokinetics of irinotecan in patients with metastatic colorectal cancer. *J Clin Oncol* **24:**3061-3068.

Tukey RH and Strassburg CP (2000) Human UDP-Glucuronosyltransferases: Metabolism, Expression, and Disease. *Annu Rev Pharmacol Toxicol* **40:**581-616.

Umar S (2010) Intestinal stem cells. *Current gastroenterology reports* **12:**340-348.

Footnotes

Financial Support: This work was supported by the National Institutes of Health grants ES010337 and GM126074 (R.H.T) and R21-AI135677 (S.C.).

The authors declare that they have no conflicts of interest with the contents of this article

DMD Fast Forward. Published on October 25, 2021 as DOI: 10.1124/dmd.121.000644
This article has not been copyedited and formatted. The final version may differ from this version.

Figure Legends

Figure 1. *Development and expression of human UGT1A1*. **(A)** Generation of mice expressing human *UGT1A1* gene in the gastrointestinal tract (*hUGT1A1^{GI}*) and liver (*hUGT1A1^{HEP}*) in a *Ugt1* null background. **(B)** RT-qPCR for *UGT1A1* in liver, small intestine (SI) and colon from *hUGT1A1^{GI}* and *hUGT1A1^{HEP}* mice (mean ± SEM; n=4). **(C)** Western Blot analysis showing tissue specific expression of UGT1A1 in different tissues of *hUGT1A1^{GI}* and *hUGT1A1^{HEP}* mice (n=2). **(D)** SN-38G formation in liver, SI and colon from *hUGT1A1^{GI}* and *hUGT1A1^{HEP}* mice (mean ± SEM;n=4). **(E)** Total Serum Bilirubin (TSB) measured in adult (8 weeks old) in *hUGT1A1^{GI}* and *hUGT1A1^{HEP}* mice (mean ± SEM; n=21). **(F)** Body weights registered in adult (8 weeks old) male and female mice (mean ± SEM; n=20 per gender and genotype). Statistical differences between groups were evaluated by One-way ANOVA, Tukey's multiple comparison test; **P < 0.01, ***P < 0.001, and ****P < 0.0001.

Figure 2. *Toxicity associated with CPT-11 administration*. Kaplan-Meier survival curves (**A**, **C**, **E** and **G**) and weight loss % (**B**, **D**, **F** and **H)** in *hUGT1A1^{GI}* and *hUGT1A1^{HEP}* mice treated with different concentrations of CPT-11 for 4 consecutive days. Age-matched adult male mice (8 weeks old) were used for these experiments (n=10). CPT-induced lethality was determined over 21 days. Body weights were monitored daily, and the weight recovery was evaluated over 15 days. Significance was assessed using unpaired Student's t test. Only significant differences are shown; *P < 0.05.

Figure 3. *Impact of CPT-11 on intestinal tissue*. *hUGT1A1^{GI}* and *hUGT1A1^{HEP}* mice (8 weeks old) were treated with either PBS or CPT-11 (10 mg/kg) for 4 consecutive days, and on day 5, small intestine (SI) samples were collected. **(A)** H&E staining from duodenum samples of *hUGT1A1^{GI}* and *hUGT1A1^{HEP}* mice. **(B)** SI length decrease (%) (mean ± SEM; n=4). **(C-E)** RT-qPCR for *Il-6*, *Il-1β* and *Cdkn1a* (mean ± SEM; n=4). **(F)** Western blot analysis on whole extract from SI (untreated n=2, treated n=3). **(G)** Band quantification of target proteins normalized to

DMD Fast Forward. Published on October 25, 2021 as DOI: 10.1124/dmd.121.000644
This article has not been copyedited and formatted. The final version may differ from this version.

GAPDH. For panes **(B-E)**, statistical differences between groups were evaluated by One-way ANOVA, Tukey's multiple comparison test; *P < 0.05 and ****P < 0.0001. For panel **(G)**, significance was assessed using Two-way ANOVA followed by Tukey's multiple comparison test; *P < 0.05, **P < 0.01 and ****P < 0.0001. Data represent at least two independent experiments. CC1, cleaved caspase 1; CC3, cleaved caspase 3; C7, caspase7; CC7, cleaved caspase 7; Cyt-c, cytochrome-c.

Figure 4. *CPT-11 treatment to organoid cultures*. **(A)** Organoid cultures isolated from *hUGT1A1*^{GI} and *hUGT1A1*^{HEP} mice. **(B)** RT-qPCR (mean ± SEM; n=3) and western blot analysis for human UGT1A1. Organoids were exposed on day 3 to CPT-11 at 0, 0.1, 1 and 10 μM for 24h. **(C-E)** RT-qPCR for *Tnfα*, *Cdkn1a*, and *Lgr5* (mean ± SEM; n=3). **(F)** Western blot analysis on whole cell extracts. **(G)** Band quantification of target proteins normalized to GAPDH. For panel **(B)**, significance was assessed using unpaired Student's t test; ****P < 0.0001. For panels **(C-E),** statistical differences between groups were evaluated by One-way ANOVA, Tukey's multiple comparison test; *P < 0.05, **P < 0.01, ***P < 0.001 and ****P < 0.0001. For panel **(G)**, significance was assessed using Two-way ANOVA followed by Tukey's multiple comparison test; *P < 0.05. Data represent at least two independent experiments. CC3, cleaved caspase 3; CC7, cleaved caspase 7; Cyt-c, cytochrome-c.

Figure 5. *Impact of ER stress on organoid cultures*. Organoids isolated from *hUGT1A1*^{GI} and *hUGT1A1*^{HEP} mice were exposed on day 3 to TGN (0, 0.01, 0.1, 1 μM) for 24h. **(A)** organoid cultures exposed to TGN (0 and 0.1 μM) and % of malformed organoids (mean ± SEM; n=3). **(B-D)** RT-qPCR for *Chop*, *Atf5*and *Lgr5* (mean ± SEM; n=3). **(E)** Western blot analysis on whole cell extracts. **(F)** Band quantification of target proteins normalized to GAPDH. For panel **(A)**, significance was assessed using unpaired Student's t test; *P < 0.05. For panels **(B-D),** statistical differences between groups were evaluated by One-way ANOVA, Tukey's multiple comparison test; *P < 0.05, **P < 0.01, ***P < 0.001 and ****P < 0.0001. For panel **(F)**, significance was assessed using Two-way ANOVA followed by Tukey's multiple comparison test; *P < 0.05; *P < 0.001. Data represent at least two independent experiments. CC3, cleaved caspase 3; CC7, cleaved caspase 7; CPT-11 (10 μM).

DMD Fast Forward. Published on October 25, 2021 as DOI: 10.1124/dmd.121.000644
This article has not been copyedited and formatted. The final version may differ from this version.

DMD Fast Forward. Published on October 25, 2021 as DOI: 10.1124/dmd.121.000644
This article has not been copyedited and formatted. The final version may differ from this version.

Figure 1

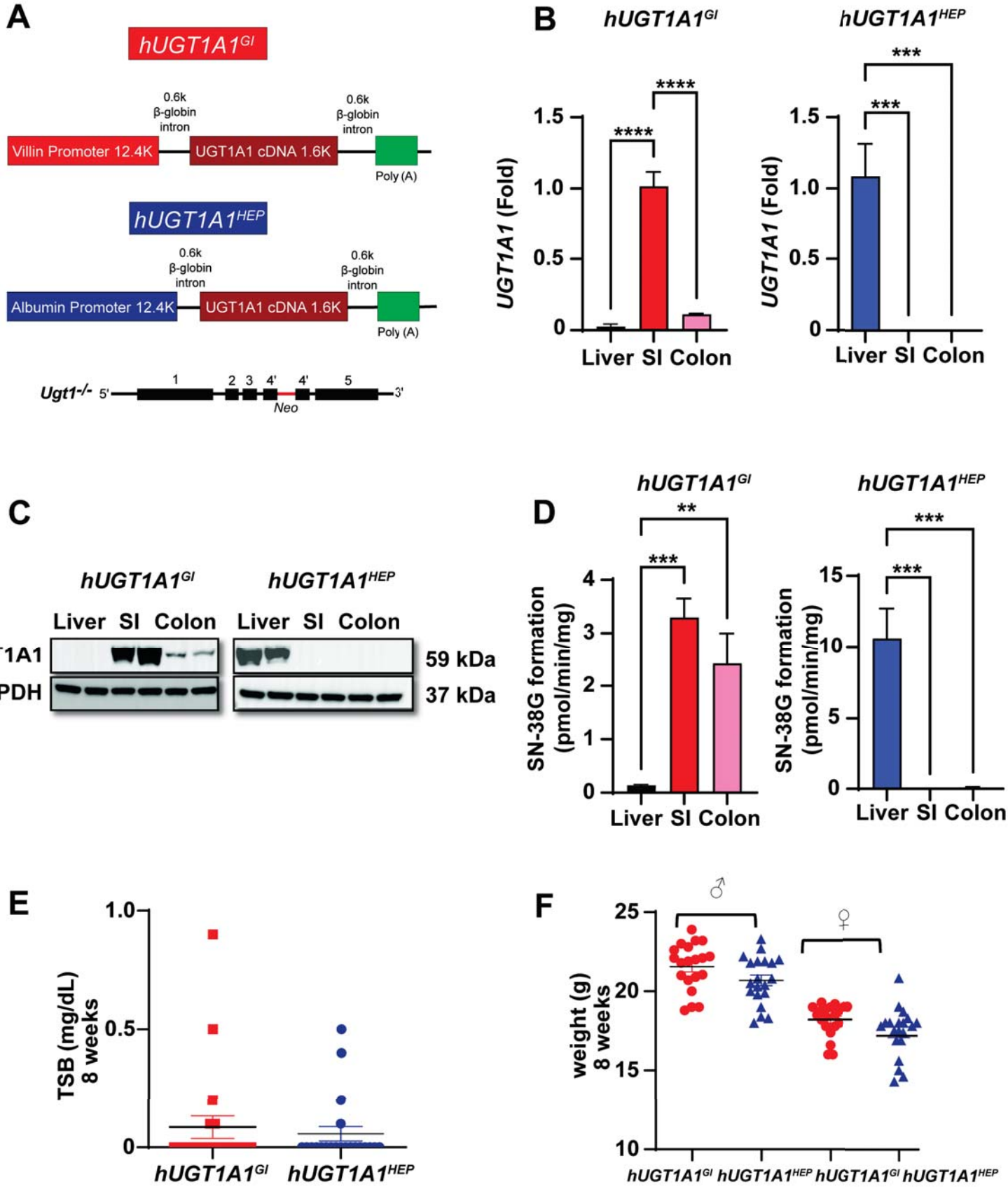

DMD Fast Forward. Published on October 25, 2021 as DOI: 10.1124/dmd.121.000644
This article has not been copyedited and formatted. The final version may differ from this version.

Figure 2

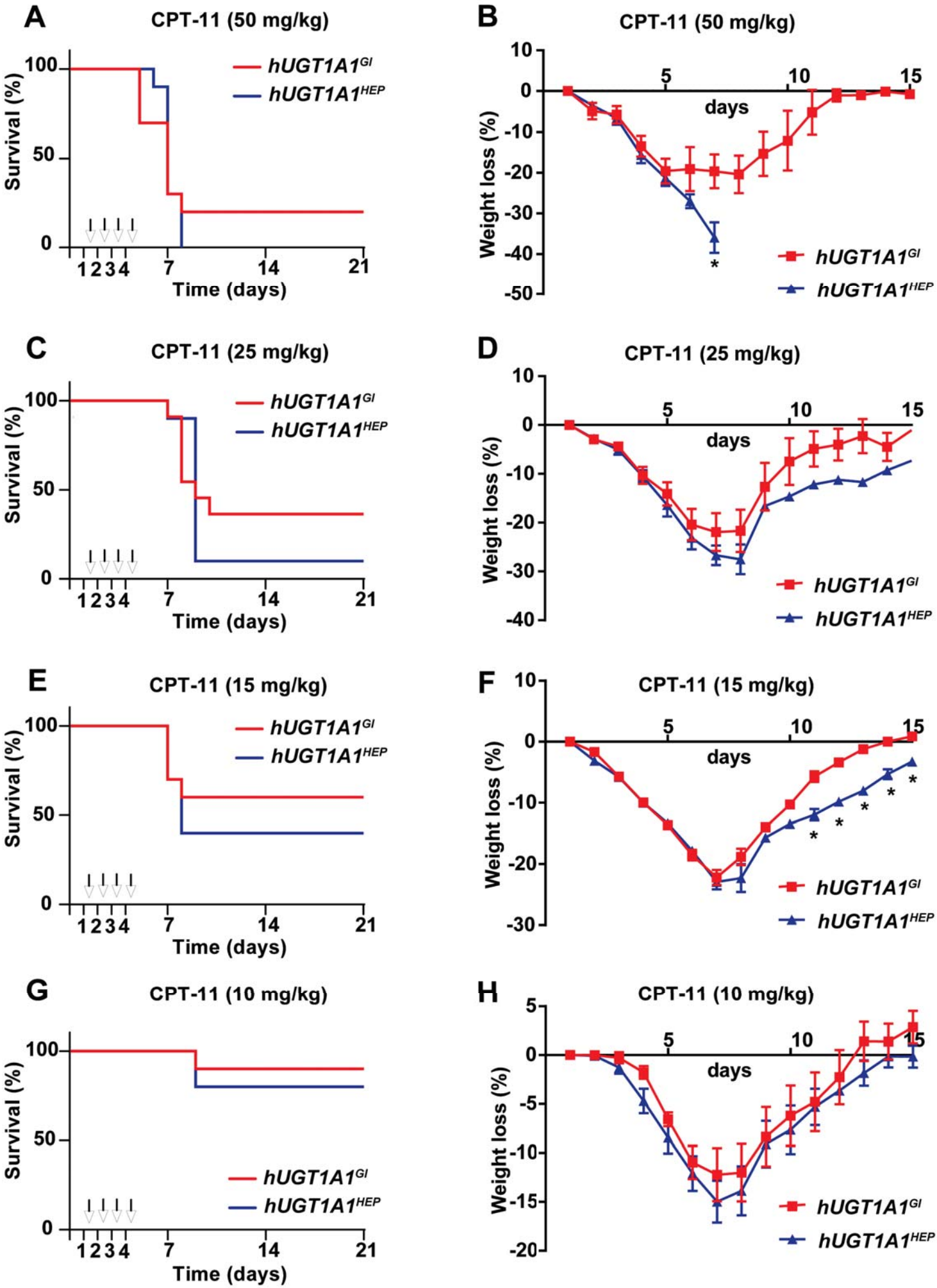

DMD Fast Forward. Published on October 25, 2021 as DOI: 10.1124/dmd.121.000644
This article has not been copyedited and formatted. The final version may differ from this version.

Figure 3

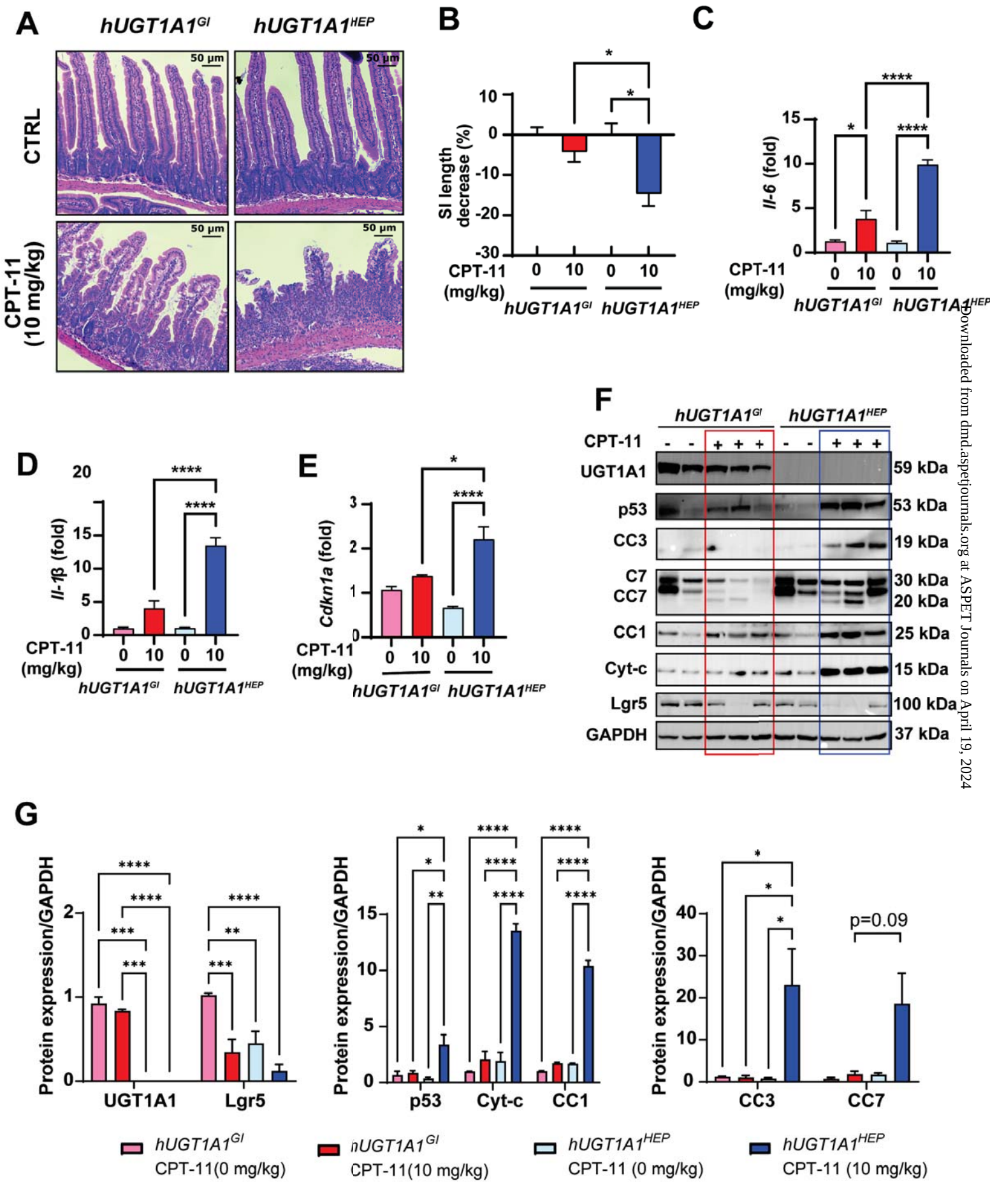

DMD Fast Forward. Published on October 25, 2021 as DOI: 10.1124/dmd.121.000644
This article has not been copyedited and formatted. The final version may differ from this version.

Figure 4

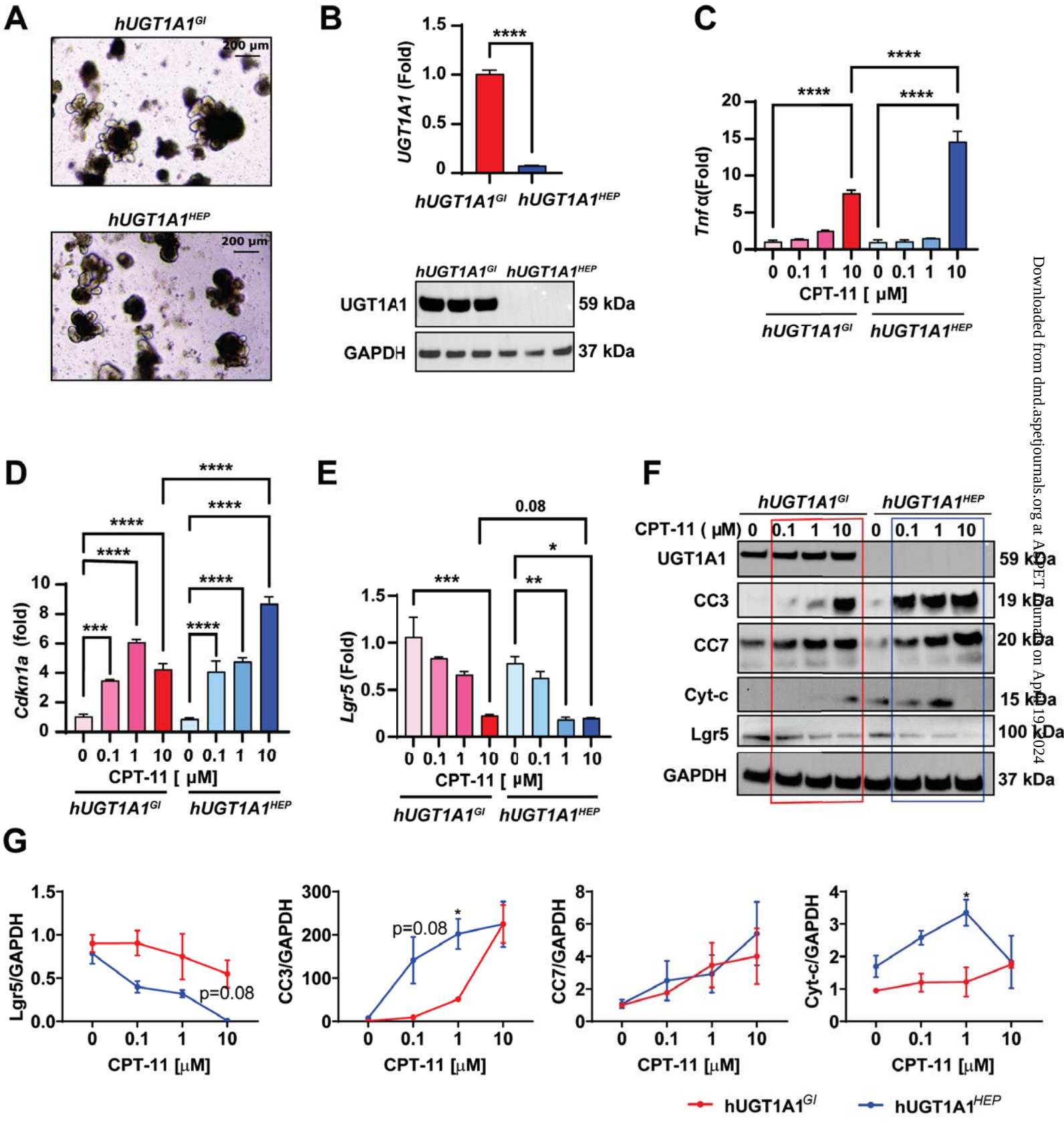

DMD Fast Forward. Published on October 25, 2021 as DOI: 10.1124/dmd.121.000644
This article has not been copyedited and formatted. The final version may differ from this version.

Figure 5

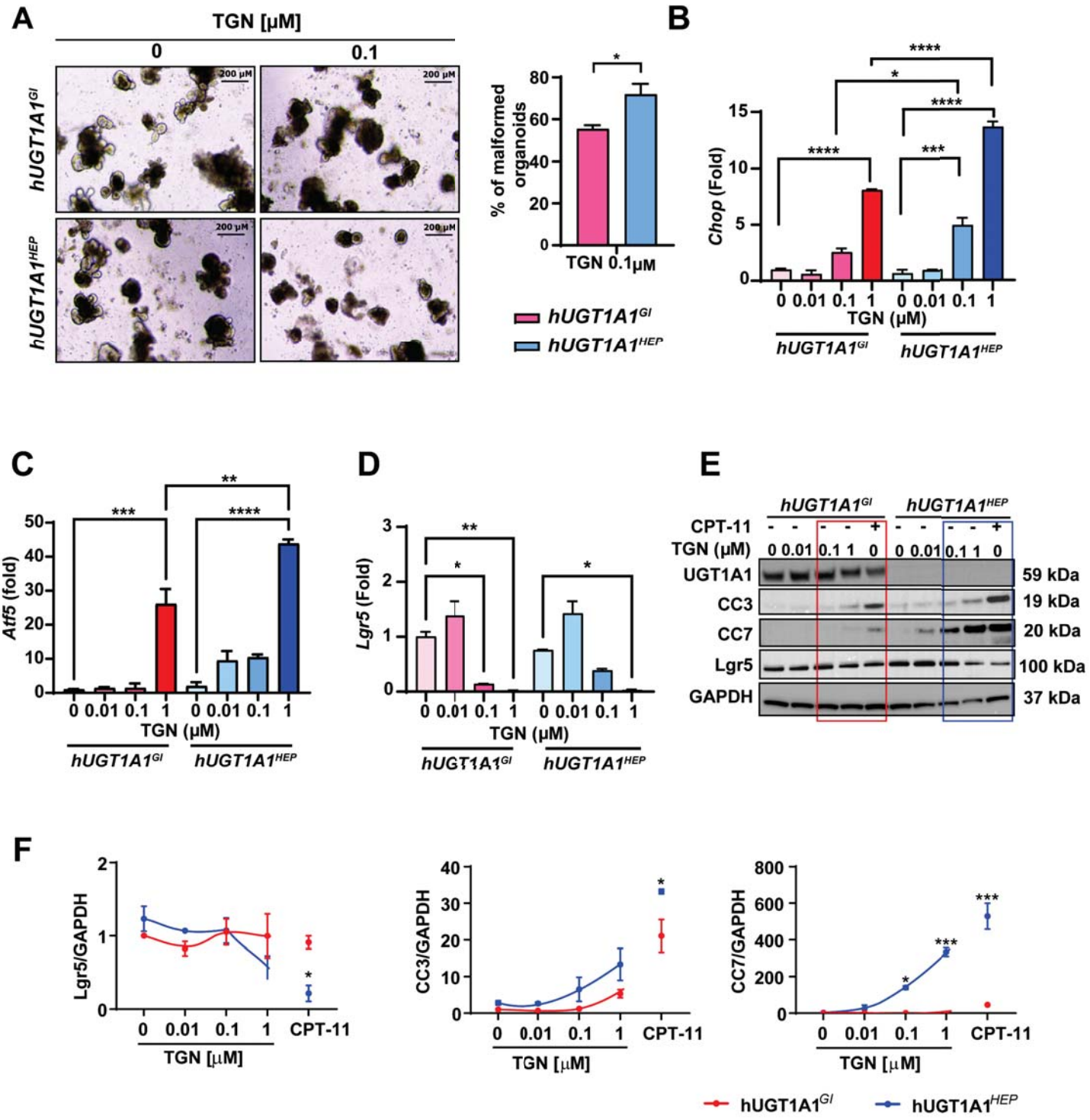

DMD-AR-2021-000644

Supplemental Information

Intestinal UGT1A1 and protection against Irinotecan-induced toxicity in a novel UGT1A1 tissue-specific humanized mouse model

Elvira Mennillo, Xiaojing Yang, Andre A. Weber, Yoshihiro Maruo, Melanie Verreault, Olivier Barbier, Shujuan Chen, Robert H. Tukey

Laboratory of Environmental Toxicology, Department of Pharmacology, University of California San Diego, La Jolla, CA 92093 (E.M, X.Y., A.A.W., S.C., R.H.T.). Department of Pediatrics, Shiga University of Medical Science, Otsu, Shiga, Japan (Y.M.). Laboratory of Moléculaire Pharmacology, Centre de Recherche du CHU de Québec, Faculté of Pharmacie, Université Laval Québec, Québec, Canada (M.V., O.B.)

Address correspondence to: Robert H. Tukey, Department of Pharmacology, University of California, San Diego, 9500 Gilman Dr., CA 92093-0722. E-mail: rtukey@health.ucsd.edu

Table S1. Primer pair sequences for genes amplified by quantitative (real-time) RT-qPCR

Gene	Primer pair sequences (5'-3')
Mouse *cph*	Fwd: ATGGTCAACCCCACCGTGT Rev:TTCTTGCTGTCTTTGGAACTTTGC
Human *UGT1A1*	Fwd: CCTTGCCTCATCAGAATTCCTTC Rev: ATTGATCCCAAAGAGAAAACCAC
Mouse *Atf5*	Fwd: TGGGCTGGCTCGTAGACTAT Rev: GTCATCCAATCAGAGAAGCCG
Mouse *Cdkn1a*	Fwd: CATTCAGAGCCACAGGCACCA Rev: CGGGACCGAAGAGACAACGG
Mouse *Chop*	Fwd: GACCAGGTTCTGCTTTCAGG Rev: CAGCGACAGAGCCAGAATAA
Mouse *Il-6*	Fwd: GAGGATACCACTCCCAACAGA Rev: AAGTGCATCATCGTTGTTCAT
Mouse *Il-1β*	Fwd: GCAACTGTTCCTGAACTCAAC Rev: ATCTTTTGGGGTCCGTCAACT
Mouse *Lgr5*	Fwd: CAGCGTCTTCACCTCCTACC Rev: TGTGTCAAAGCATTTCCAGC
Mouse *Tnfα*	Fwd: GATCGGTCCCCAAAGGGATG Rev: GGCTACAGGCTTGTCACTCG

Figure S1. (A) Total Serum Bilirubin (TSB) levels in *Ugt1*$^{-/-}$, *hUGT1A1*^{GI} and *hUGT1A1*^{HEP} mice at different days post birth (7, 14 and 21). **(B)** Western blot analysis for human UGT1A1 in whole extracts obtained from small intestine (SI) of *hUGT1A1*^{GI} mice and liver of *hUGT1A1*^{HEP} mice and relative expression of UGT1A1/GAPDH.